Resonant spin tunneling in randomly oriented nanospheres of Mn_{12} acetate

S. Lendínez, R. Zarzuela, J. Tejada, M. W. Terban, S. J. L. Billinge, J. Espin, I. Imaz, D. Maspoch, and E. M. Chudnovsky

Resonant Spin Tunneling in Randomly Oriented Nanospheres of Mn_{12} Acetate

S. Lendínez, R. Zarzuela, J. Tejada

Departament de Física Fonamental, Facultat de Física,
Universitat de Barcelona, Martí i Franquès 1, 08028 Barcelona, Spain

M. W. Terban[1], S. J. L. Billinge[1,2]

[1]*Department of Applied Physics and Applied Mathematics,*
Columbia University, New York, NY 10027, USA
[2]*Condensed Matter Physics and Materials Science Department,*
Brookhaven National Laboratory, Upton, NY 11973, USA

J. Espin[1], I. Imaz[1], D. Maspoch[1,2]

[1]*Institut Català de Nanotecnologia, ICN2, Esfera Universitat*
Autónoma Barcelona (UAB), Campus UAB, 08193 Bellaterra, Spain
[2]*Institució Catalana de Recerca i Estudis Avançats (ICREA), 08100 Barcelona, Spain*

E. M. Chudnovsky

Physics Department, Lehman College, The City University of New York,
250 Bedford Park Boulevard West, Bronx, NY 10468-1589, USA
(Dated: December 19, 2014)

We report measurements and theoretical analysis of resonant spin tunneling in randomly oriented nanospheres of a molecular magnet. Amorphous nanospheres of Mn_{12} acetate have been fabricated and characterized by chemical, infrared, TEM, X-ray, and magnetic methods. Magnetic measurements have revealed sharp tunneling peaks in the field derivative of the magnetization that occur at the typical resonant field values for the Mn_{12} acetate crystal in the field parallel to the easy axis. Theoretical analysis is provided that explains these observations. We argue that resonant spin tunneling in a molecular magnet can be established in a powder sample, without the need for a single crystal and without aligning the easy magnetization axes of the molecules. This is confirmed by re-analyzing the old data on a powdered sample of non-oriented micron-size crystals of Mn_{12} acetate. Our findings can greatly simplify the selection of candidates for quantum spin tunneling among newly synthesized molecular magnets.

I. INTRODUCTION

Spin tunneling in molecular magnets has been subject of intensive research in the last 20 years[1,2]. These systems exhibit unique quantum features that show up in macroscopic experiments. Among them are step-wise quantum hysteresis due to resonant tunneling at discrete values of the magnetic field[3–5], topological Berry phase effects[6], magnetic deflagration[7,8], and Rabi oscillations[9,10]. Most recently, experiments with individual magnetic molecules bridged between conducting leads and molecules grafted on carbon nanotubes have been performed that permit readout of quantum states of individual atomic nuclei[11,12]. Quantum superposition of spin states in magnetic molecules makes them candidates for qubits – elements of quantum computers[13].

Beginning with the discovery of resonant spin tunneling in Mn_{12} acetate[3] it has been generally believed that at the macroscopic level the effect can only be observed in a single crystal or in the array of microcrystallites whose crystallographic axes are aligned. The latter method was used in Refs. 3,4, and in a few subsequent publications by the same authors, before sufficiently large single crystals of molecular magnets had become available. Nowadays a large number of new molecular magnets are synthesized by chemists every year and subsequently tested by physicists for the presence of spin tunneling. In many cases growing a sufficiently large single crystal is a challenging task as compared to growing microcrystals. At the same time the effectiveness of the room-temperature alignment of microscrystals by a high magnetic field in, e.g., an epoxy, strongly depends on the shape of the crystallites and may also be incompatible with their chemistry.

In this paper we show that neither macroscopic single crystals or the alignment of microcrystals are necessary to obtain solid evidence of spin tunneling in macroscopic magnetic measurements of molecular magnets. This can be done by simply measuring the magnetization curve, $M(H)$, and plotting the derivative of the magnetization on the magnetic field, dM/dH. To illustrate this point we use amorphous nanospheres of Mn_{12} acetate[14,15]. Such nanospheres neither form crystals nor they allow to align easy magnetization axes of Mn_{12} molecules in a high magnetic field because of their isotropic magnetic susceptibility.

First magnetic measurements of similar Mn_{12} nanoparticles were performed in Refs. 14,15 where peaks in dM/dH were observed and attributed to quantum tun-

neling. However, no explanation to such observation in a disordered sample has been provided. Zero-field cooled magnetization curve of the measured sample revealed large, up to 40%, fraction of fast-relaxing species of Mn_{12} acetate. This resulted in a complicated pattern of displaced tunneling maxima as compared to typical resonances in a Mn_{12} crystal, in the field parallel to the easy axis, that are separated by about 4.6 kOe.

Highly amorphous Mn_{12} particles used in our experiments did not show any visible presence of the second species. Sharp tunneling maxima in dM/dH have been observed. Their location coincided with the position of tunneling maxima in a Mn_{12} crystal. We provide theoretical analysis that explains observation of tunneling resonances in a fully disordered sample. The predicted postresonance field dependence of the peaks agrees with experiment. The practical value of this observation is that it can greatly reduce the preliminary work by chemists that is required to search for quantum spin tunneling in newly synthesized molecular magnets. As long as the magnetic molecules preserve their structure, the disordered sample of crystallites of any size is sufficient for that task. This was previously shown by the studies of zero-field magnetic relaxation in Mn_{12} clusters frozen in solutions[16] and in highly disordered samples of Mn_{12} benzoate[17].

The paper is structured as follows. Fabrication and characterization of the samples by various techniques are discussed in Section II. Measurements of the field and temperature dependence of the magnetization, and of the ac susceptibility, are presented in Section III. They are analyzed and explained in Section IV. Section V summarizes our results and offers some final remarks.

II.   FABRICATION AND CHARACTERIZATION OF MN_{12} NANOSPHERES

To obtain spherical Mn_{12} acetate particles showing the highest degree of amorphous character they were synthesized using a method adapted from the earlier publication[14]. In a typical experiment, 60 mg of Mn_{12} acetate were dissolved in 15 mL of acetonitrile. The solution was added to 30 mL of toluene under vigorous stirring. Precipitation of a brown solid was observed. One hour later the resulting dispersion was centrifuged ($4' \times 8000$ rpm) and the supernatant was collected. The pellet was redispersed with acetonitrile:toluene (1 : 2), centrifuged again and the supernatant was collected again. Both supernatants were then mixed and dried under vacuum condition. 5.8 mg of a brown solid (10% yield) were collected and stored in vacuum.

Scanning and Transmission Electron Microscopy (SEM and TEM) images of the brown solid revealed the formation of uniform spherical particles, see Fig. 1. The size of the particles was calculated from FESEM images by averaging the diameter of at least 300 particles from different areas of the sample. The average size of 237
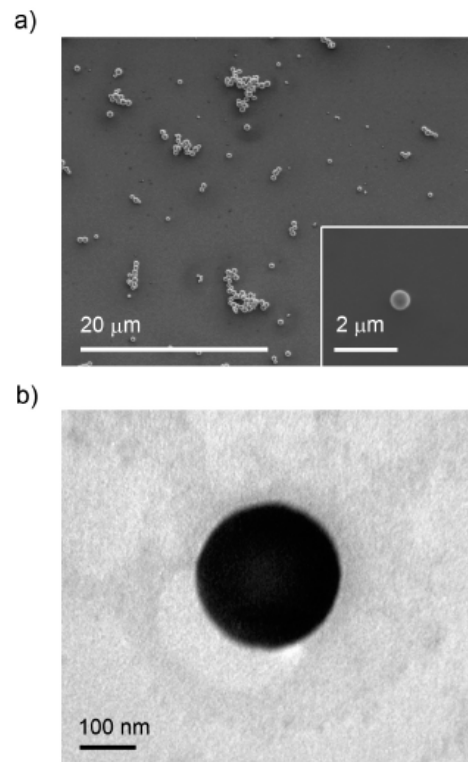

Figure 1: a) Representative SEM image of Mn_{12} acetate spherical particles. Inset: individual particle. b) TEM image of an individual Mn_{12} acetate nanosphere.

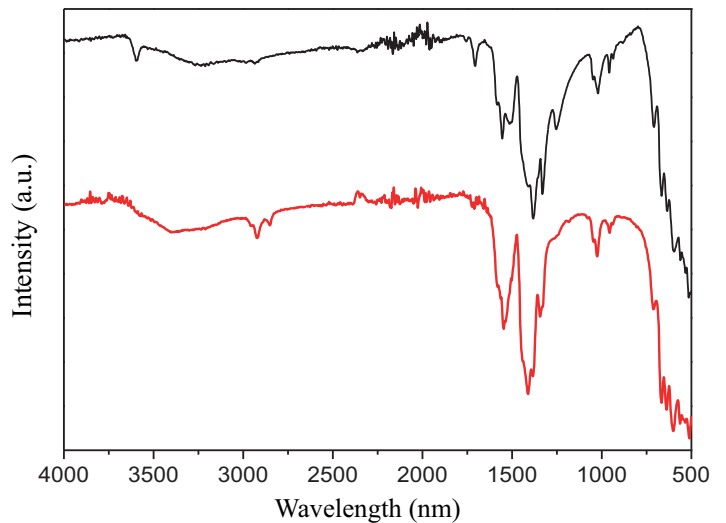Figure 2: Color online: IR spectra of bulk Mn_{12} acetate crystals (black) and amorphous Mn_{12} acetate nanospheres (red).

± 69 nm and the median size of 238 nm were determined. This average size was further confirmed by dynamic light scattering (DLS). The chemical correspondence with bulk $[Mn_{12}O_{12}(CH_3COO)_{16}(H_2O)_4]$ crystals was confirmed by elemental analysis and by the positive matching between the IR spectra, see Fig. 2. As we shall see below, the additional evidence of the conventional structure of Mn_{12} molecules in the nanospheres follows from the magnetic measurements that reveal the resonant spin tunneling at the same values of the magnetic field as for the single crystals of Mn_{12} acetate.
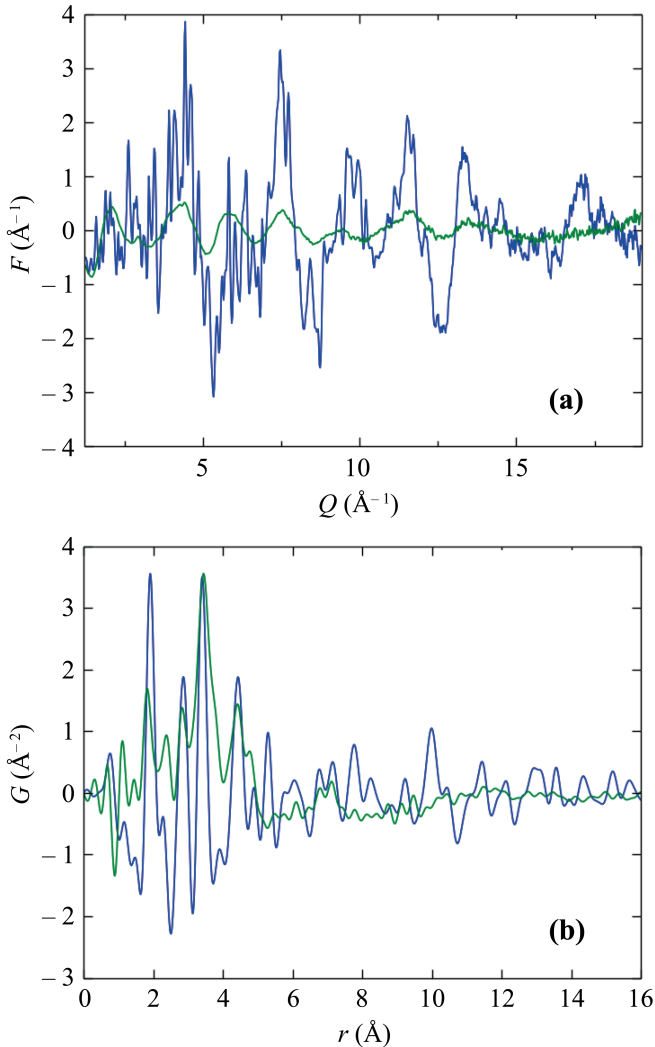

Figure 3: Color online: (a) Structure factors for microscrystals (blue) and nanospheres (green) of Mn_{12} acetate. (b) Superimposed pair distribution functions for microscrystals (blue) and nanospheres (green) of Mn_{12} acetate.

To confirm the amorphous character of spherical Mn_{12} particles, X-ray studies have been conducted on a beam-line X17A at the National Synchrotron Light Source at Brookhaven National Laboratory. Scattering intensity was measured from high energy X-rays at an energy of 67.419 keV using the rapid acquisition pair distribution function (RAPDF) technique[18,19]. A large area 2-D Perkin Elmer detector with 2048×2048 pixels and 200×200 μm pixel size was mounted orthogonal to the beam path with a sample-to-detector distance of 206.1371 mm. Two samples have been measured for comparison: The sample of conventionally grown alongated micron-size crystallites of Mn_{12} acetate and the sample of Mn_{12} nanospheres described above.

Structure factors and pair distribution functions for the two samples are shown in Fig. 3. While distinct Bragg picks of Mn_{12} acetate[20,21] are present in the microcrystalline sample, a very diffused intensity has been found in the nanospheres. Same differences have been observed in the RAPDF, indicating high level of disorder in the nanospheres. They must be either extremely defected or amorphous. As we shall see from magnetic measurements, however, the Mn_{12} molecules are well preserved in the nanospheres despite of the structural disorder.

Amorphous or highly disordered structure of Mn_{12} nanospheres raises the question whether the easy axes of Mn_{12} molecules inside the spheres are aligned or disordered. One should notice in this connection that the direction of the easy axis is related to the orientation of the molecules while the Bragg peaks in the X-ray scattering are related to the translational order in a crystal. In an amorphous solid the orientation of local crystallographic axes is more robust than the translational order[22]. It may spread well beyond the amorphous structure factor. Evidence of the extended correlations in the orientation of local magnetic anisotropy axes has been previously reported in amorphous magnets[23].

In principle, spectroscopic studies of disordered samples, such as high-frequency electron spin resonance (HFESR) and frequency-domain magnetic-resonance spectroscopy (FDMRS), combined with theoretical models that incorporate the effects of disorder and dipolar broadening on spin tunneling, may shed light on the structure of magnetic clusters and the orientation of easy axis, as has been demonstrated in Ref. 17 for nearly amorphous samples of Mn_{12} benzoate. Similar information has been obtained in Ref. 24 for a partially ordered sample of magnetic molecules deposited on surfaces by using synchrotron-based spectroscopic techniques combined with the study of angular dependence of the magnetic hysteresis and theoretical modeling. Such analysis is rather involved and depends on the model of disorder. For the conclusions made in this paper it does not matter whether the easy axes of the molecules are disordered at the level of individual nanospheres, or due to the random orientation of nanospheres, or both.

III.   MAGNETIC MEASUREMENTS

Low-temperature magnetic measurements have been carried out on a compressed powdered sample inside a

commercial rf-SQUID Quantum Design magnetometer. Before conducting the measurements, an attempt has been made to orient the nanoparticles by a high magnetic field at room temperature in the epoxy, as has been done previously with μm-size microcrystals. Contrary to the latter case, the orienting procedure applied to the nanospheres rendered no difference in the magnetization data. This can be understood from the fact that micronsize crystallites of Mn_{12} acetate grow elongated along the easy magnetization axis. The resulting anisotropy of their magnetic susceptibility then enables the alignment of the crystallites by a high magnetic field in a Stycast, even though the molecules do not have magnetic moments at room temperature. This method, however, does not work for the Mn_{12} nanoparticles of spherical shape.
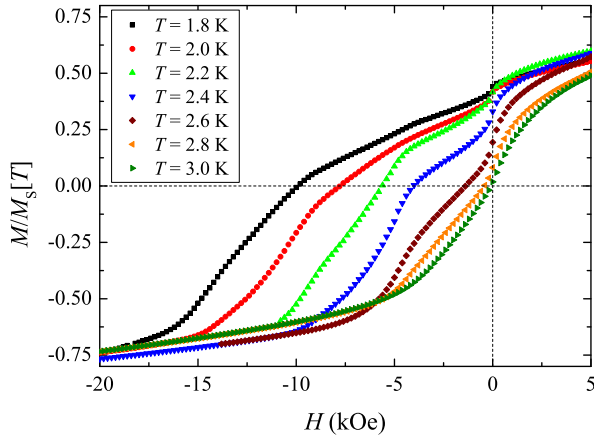

Figure 4: Color online: $H < 0$ branch of the hysteresis curves of the disordered powder of Mn_{12} nanospheres at different temperatures.

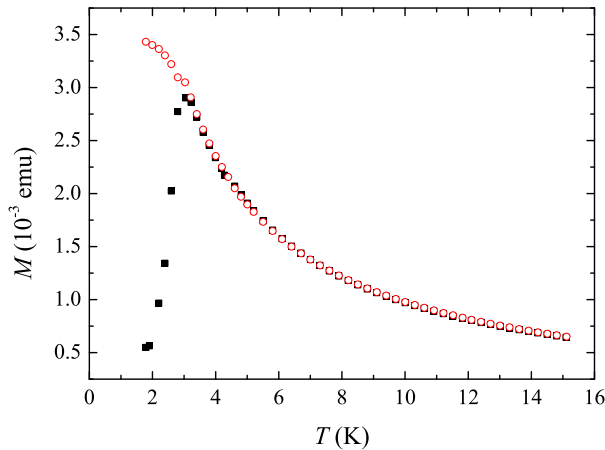Figure 5: Color online: Field-cooled (FC) and zero-field-cooled (ZFC) magnetization vs temperature curves for a disordered powder of Mn_{12} nanospheres in the dc field of 100 Oe.
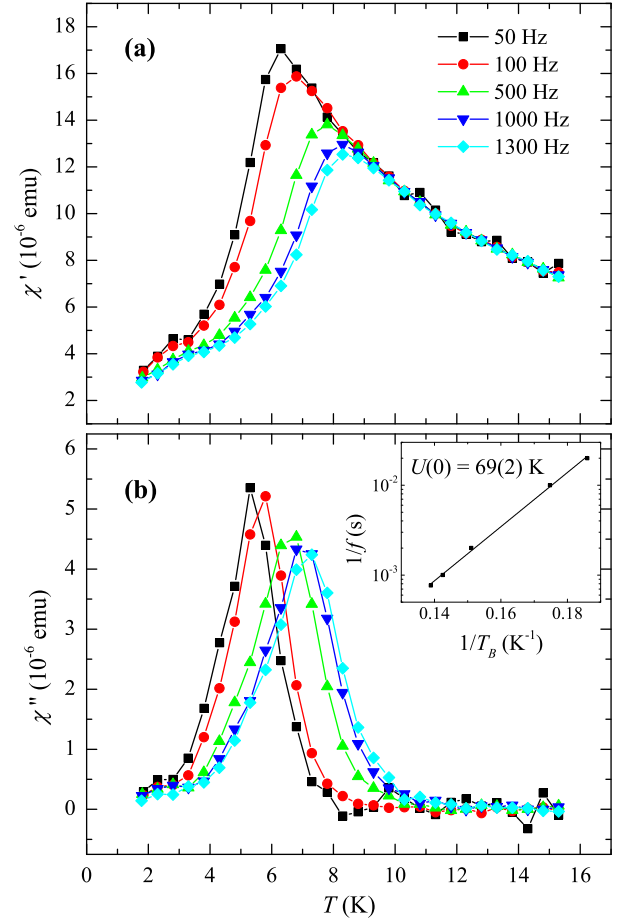
Negative branches of hysteresis curves are shown in

Figure 6: Color online: Real part (a) and imaginary part (b) of the ac susceptibility in the frequency range $f = 50$ Hz - 1.3 kHz in the presence of a 3 Oe ac field. The inset shows logarithmic dependence of the blocking temperature on $1/f$. The fitted value of the energy barrier in a zero field is $U(0) = 69 \pm 2$ K.

Fig. 4. At the lowest temperature used, when thermal effects are weak, $M(0)$ is about one half of the saturation value, M_S. This corresponds to the magnetic moments of Mn_{12} molecules looking randomly into a hemisphere, which follows from

$$\frac{M(0)}{M_S} = \frac{1}{4\pi} \int_0^{2\pi} \mathrm{d}\phi \int_0^{\pi/2} \sin\theta \mathrm{d}\theta = \frac{1}{2}. \qquad (1)$$

The latter is true regardless of whether the disorder in the orientation of easy magnetization axes occurs at the level of individual Mn_{12} molecules inside amorphous nanospheres or at the level of the nanospheres, each having a coherent orientation of the easy axes of the molecules.

Field-cooled (FC) and zero-field-cooled (ZFC) magnetization curves are shown in Fig. 5. High-temperature behavior is a $1/T$ Curie law. Fig. 6 shows the ac susceptibility of the Mn_{12} nanospheres. The maximum in both families of curves occurs at the blocking temperature,

T_B, determined by the magnetic moments that reverse their orientation on the time scale of the measurement, $t = t_0 \exp[U(H)/T_B]$, with t_0 being the attempt time and $U(H)$ being the energy barrier. In the ac measurements $t \sim 1/f$, so that T_B scales with the frequency of the ac field as $U(H)/\ln(1/t_0 f)$, which is in accordance with the data, see the inset in Fig. 6b. The estimated values for the attempt time and the energy barrier at zero field are $t_0 = (5 \pm 1) \times 10^{-8}$ s and $U(0) = 69 \pm 2$ K, respectively.

One-maximum structure of the curves shown in Figs. 5 and 6 contrasts with a pronounced two-maxima structure observed in Refs. 14,15, with the second, lower maximum occurring at a lower temperature. The latter, according to the authors of Refs. 14,15, where spherical nanoparticles of average size under 50 nm were studied, corresponded to the presence of 40% fast-relaxing species of Mn_{12} acetate. If such a species were present in our highly amorphous, larger spherical particles, it would have had a very low abundance. This simplifies the analysis of the data presented in the next section.
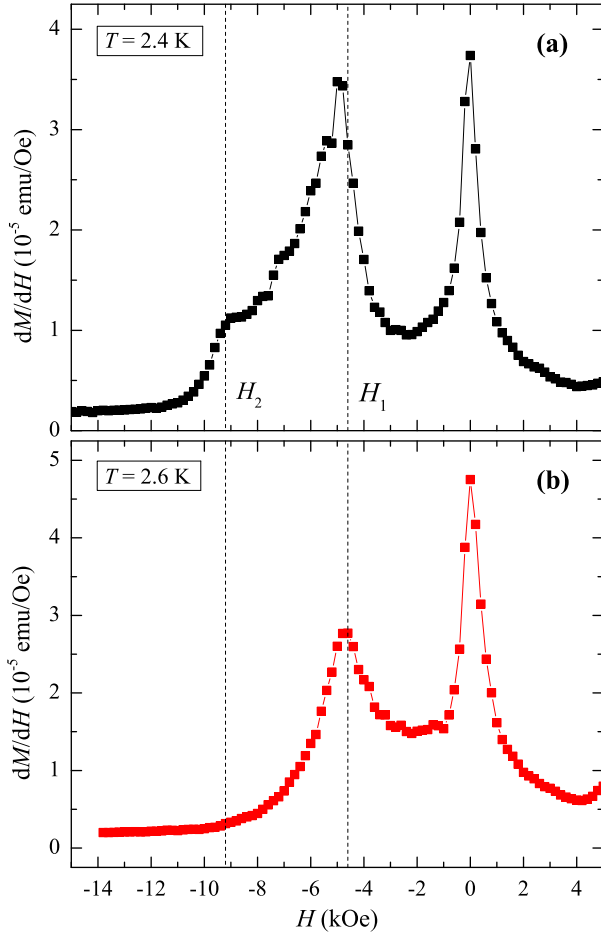

Figure 7: Color online: dM/dH for the $H < 0$ branch of the hysteresis curve of the disordered powder of Mn_{12} acetate nanospheres: (a) $T = 2.4$ K, (b) $T = 2.6$ K.

Fig. 7 shows the derivative, dM/dH, along the negative branch of the hysteresis curve shown in Fig. 4, for

two temperatures. The observed zero-field maximum has the width of about 1 kOe and is much more narrow than the zero-field maximum observed in Refs. 14,15. There are clear maxima at $H_1 \approx 4.6$ kOe and $H_2 \approx 9.2$ kOe as in a Mn_{12} acetate crystal in the field parallel to the easy axis.

IV.   ANALYSIS OF THE MAGNETIZATION DATA

At first glance, the presence of the maxima in the dM/dH plot, Fig. 7, that correlate with the typical tunneling maxima of Mn_{12} acetate in the field parallel to the easy axis, that occur at $H_n = nH_1$, with $H_1 \approx 4.6$ kOe, is surprising given the random orientation of the easy magnetization axes of the molecules. Simple analysis presented below shows however that the tunneling maxima can and should be observed in dM/dH obtained from a sample of randomly oriented magnetic molecules. Let us look closer at the magnetization curve in Fig. 4 that corresponds to the sweep from a positive to a negative field.
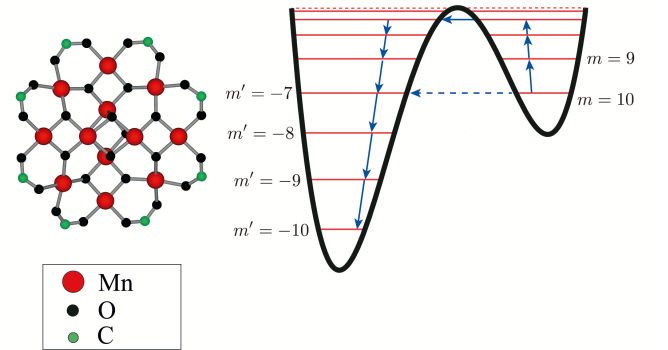

Figure 8: Thermally assisted tunneling between resonant spin levels in a Mn_{12} molecule. The black solid curve shows the dependence of the classical magnetic anisotropy energy on $\cos\theta$. Red lines show energies of spin levels corresponding to magnetic quantum numbers m and m'. The dash line illustrates quantum tunneling from $m = 10$ to $m' = -7$ at $H = H_3$.

Thermally assisted spin tunneling illustrated by Fig. 8 takes place as the field becomes opposite to the magnetization, $H < 0$. If the easy axis of a particular molecule makes the angle θ with the negative direction of the field, then the condition of the n-th resonance is

$$H = -\frac{H_n}{\cos\theta}, \quad 0 \leq \theta \leq \frac{\pi}{2} \tag{2}$$

Thus, at any value of the field H the molecules that are on the n-th resonance satisfy

$$\cos\theta = -\frac{H_n}{H} \tag{3}$$

The zero-field maximum in dM/dH that has been observed in all cases has an obvious explanation. At $H = 0$ all molecules are close to the $n = 0$ resonance up to the detuning effect of local dipolar and hyperfine fields that provide the finite width of the zero-field resonance. The latter is of the order of 1 kOe or below. Here we focus on the subsequent resonances $n = 1, 2, ...$ that have not been reported for disordered powders in the past.

Since the element of the spherical volume is proportional to $\sin\theta d\theta = -d\cos\theta$, the total number of molecules that enter the resonance condition when the field increases in the negative direction by a small increment $dH < 0$ is

$$dN_{\text{res}} \propto -d\cos\theta \propto -\frac{dH}{H^2} \sum_{H_n \leq |H|} H_n > 0 \qquad (4)$$

At low temperature, when the field sweep is sufficiently slow, the change in the magnetization, dM, should be proportional to $-dN_{\text{res}}$,

$$dM \propto -dN_{\text{res}} \propto \frac{dH}{H^2} \sum_{H_n \leq |H|} H_n < 0. \qquad (5)$$

This gives

$$\frac{dM}{dH} \propto \frac{1}{H^2} \sum_{H_n \leq |H|} H_n > 0 \qquad (6)$$

The function in the right-hand-side of this equation has a jump-wise behavior. At $H_1 \leq |H| < H_2 = 2H_1$ it behaves as H_1/H^2. At $H_2 \leq |H| < H_3 = 3H_1$ it behaves as $3H_1/H^2$. At $H_3 \leq |H| < H_4 = 4H_1$ it behaves as $6H_1/H^2$, and so on. Its value at $H = H_n$ equals

$$\frac{1}{H_n^2} \sum_{H_n \leq |H|} H_n = \frac{1}{n^2 H_1} \sum_{k=1}^{n} k = \frac{1}{2H_1}\left(1 + \frac{1}{n}\right). \qquad (7)$$

This analysis leads to the following conclusion. Spin tunneling resonances in a system of randomly oriented magnetic molecules can be seen as maxima in dM/dH. However, only the $H = 0$ maximum is a narrow tunneling resonance for all molecules within dipolar/hyperfine window. Each subsequent n-th "resonance" begins at $H = -H_n$ and extends to all $H < -H_n < 0$ due to different resonance conditions for differently oriented molecules. If one neglects broadening due to dipolar and hyperfine fields, these "resonances" begin with a vertical jump in dM/dH at $H = -H_n$, followed by the $1/H^2$ decrease of dM/dH. Dipolar and hyperfine fields must smear the initial vertical rise of the "resonance" by up to 1 kOe. However, the $1/H^2$ post-resonance ($H < -H_n$) decrease of dM/dH over the 4.6 kOe range from $H = -H_n$ to $H = -H_{n+1}$ must be apparent. This is seen in Fig. 9 that shows the fit of the post-resonance dM/dH by $1/H^2$ after crossing the first resonance. In the kelvin temperature range quantum effects become less pronounced at higher temperatures and higher n due to the exponential increase of thermal relaxation on temperature and
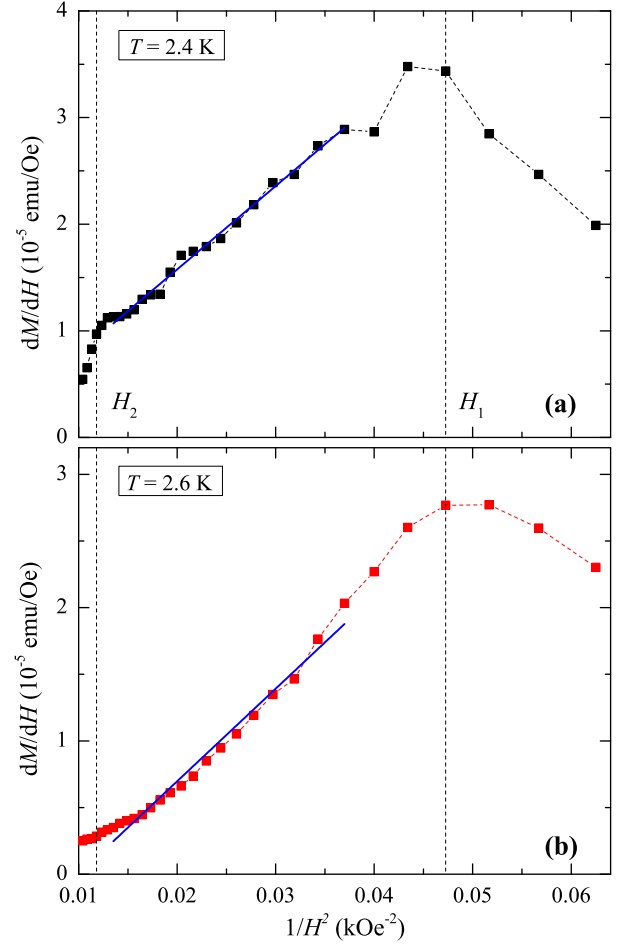

Figure 9: Color online: The $1/H^2$ fit (blue line) of dM/dH between first and second spin tunneling resonances for a disordered powder of Mn_{12} nanospheres: (a) $T = 2.4$ K, (b) $T = 2.6$ K.

on lowering the barrier by the field. This sensitivity to temperature and field must be especially strong as T approached the $H = 0$ dc blocking temperature of 3K, which is seen in experiment.

Note that for the same reason as discussed above the evidence of spin tunneling in a disordered system can also be obtained by plotting the dependence of the blocking temperature on the dc magnetic field, see Fig. 10. The blocking temperature, T_B, is proportional to the energy barrier for the spin reversal, $U(H)$. At $H = 0$ the barrier is lowered due to thermally assisted quantum tunneling between resonant spin levels near the top of the barrier, see Fig. 8. The number of molecules on the zero-field resonance at a particular value of the field progressively drops as the field approaches the boundary of the dipolar/hyperfine window, which for Mn_{12} has a width of the order of 1 kOe. At that boundary T_B is approximately determined by the full 69 K classical energy barrier for the superparamagnetic spin flip. As the field continues to increase, the field dependence of the blocking tem-
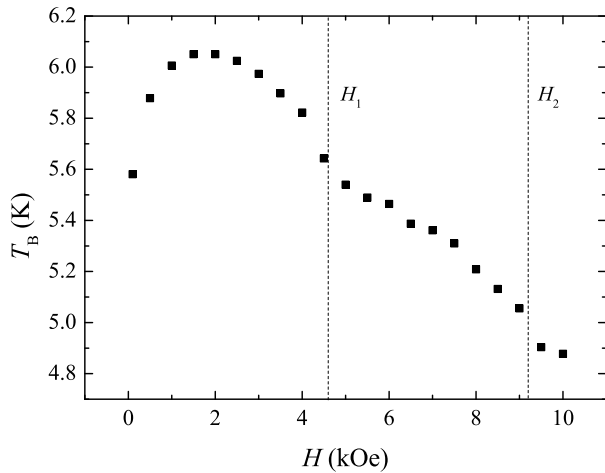
Figure 10: Color online: Dependence of the blocking temperature on the dc field in the ac field of 100 Hz.

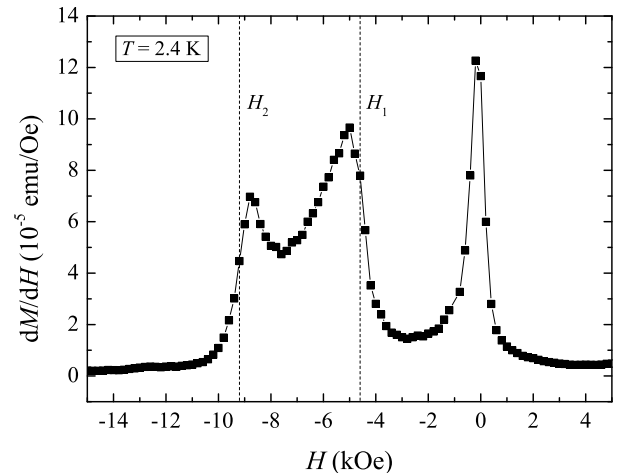Figure 11: Color online: Field derivative of the magnetization in a sample of randomly oriented micron-size crystallites of Mn_{12} acetate.

perature is dominated by the classical reduction of the energy barrier due to the growing Zeeman energy, which leads to the decrease of T_B on H. When the field reaches $H_1 \approx 4.6$ kOe, randomly oriented Mn_{12} molecules begin to enter the first resonance. The evidence of that is clearly seen in Fig. 10 in the change of the derivative of T_B on H at $H = H_1$.

V.   DISCUSSION

We have studied spin tunneling effects in amorphous nanospheres of Mn_{12} acetate. Samples have been characterized by chemical, infrared, TEM, X-ray, and magnetic methods. While the structure of Mn_{12} molecules appears to be the same as in a crystalline sample, their easy magnetization axes are completely disordered. Random orientation of the easy axes has been confirmed by magnetic measurements. It occurs either at the level of individual molecules inside the nanospheres, or at the level of randomly oriented nanospheres, or both. Isotropic magnetic susceptibility of the nanospheres at room temperature, when Mn_{12} molecules do not possess magnetic moments, excludes any possibility of aligning their easy axes in a high magnetic field as was done for the sample of Mn_{12} acetate consisting of elongated microcrystals[3].

Measurements of the FC and ZFC magnetization curves, and of the ac susceptibility, revealed presence of only one magnetic species of Mn_{12} acetate, which is in contrast with previous measurements on nanospheres containing comparable amounts of slow and fast relaxing species[14,15]. The striking feature of the magnetization curve is the presence of well-defined sharp tunneling maxima in dM/dH in a sample with random orientation of easy magnetization axes of the molecules. The maxima occur at the conventional resonant fields for the Mn_{12} acetate crystal in the field parallel to the easy axis, $H_n = -nH_1$, with $H_1 \approx 4.6$ kOe.

Quantitative explanation to this observation is provided. At any value of the field H the molecules that are on the n-th resonance have their easy axis at an angle θ with the field, satisfying $\cos\theta = -H_n/H$. Thus, as soon as the field enters the range $H \leq -H_n$ a new set of molecules that satisfy the n-th resonance condition begins to reverse their magnetization. This results in the change of the slope of $M(H)$ every time when the field reaches the value $H_n = -nH_1$, and in the corresponding peaks in dM/dH. However, only the $n = 0$ peak is the same tunneling resonance as in a crystalline sample, when all molecules achieve the resonance condition inside the dipolar/hyperfine field window. As our analysis show, all subsequent resonances are characterized by a steep jump of dM/dH at $H_n = -nH_1$ followed by a $1/H^2$ decrease. This conclusion agrees with the experimental data.

Inevitably, our findings raise the following question. Is the effort to grow a single crystal or the laborious procedure of aligning microcrystals, as was done in Ref. 3 that reported the discovery of the resonant spin tunneling in Mn_{12} acetate, really necessary to obtain the evidence of spin tunneling? As has been illustrated by this paper, the answer is apparently no. One can also make another useful statement: When a system of magnetic molecules exhibits tunneling maxima in dM/dH, it does not necessarily mean that the easy axes of the molecules are ordered. To further illustrate this point we conducted measurements of the non-oriented powder of micron-size crystals identical to the powder used in Ref. 3 where microcrystals were oriented in an epoxy prior to taking magnetic measurements. The dM/dH plot obtained from the powder sample without any orientation effort is presented in Fig. 11. It clearly shows three tunneling maxima.

We, therefore, conclude that while single crystals are good for the in depth study of spin tunneling, the robust evidence of the effect can be obtained from the magne-

tization curve of any disordered micro-crystalline sample as long as the magnetic molecules preserve their structure. This should greatly simplify the effort by chemists and physicists to track spin tunneling effects in newly synthesized molecular magnets.

VI. ACKNOWLEDGEMENTS

[1] E.M. Chudnovsky and J. Tejada, *Macroscopic Quantum Tunneling of the Magnetic Moment*, (Cambridge University Press, Cambridge, England, 1998).

[2] Recent book: *Molecular Magnets – Physics and Applications*, Ed. by J. Bartolomé, F. Luis., and J. F. Fernández, (Springer, 2014, Heidelberg New York Dordrecht London; DOI: 10.1007/978-3-642-40609-62014).

[3] J.R. Freedman, M.P. Sarachik, J. Tejada, and R. Ziolo, Phys. Rev. Lett. **76**, 3830 (1996).

[4] J.M. Hernandez, X.X. Zhang, F. Luis, J. Bartolome, J. Tejada, and R. Ziolo, Europhys. Lett. **35**, 301 (1996).

[5] L. Thomas, Fl. Lionti, R. Ballou, D. Gatteschi, R. Sessoli, and B. Barbara, Nature London **383**, 145 (1996).

[6] W. Wernsdorfer and R. Sessoli, Science **284**, 133 (1999).

[7] Y. Suzuki, M.P. Sarachik, E.M. Chudnovsky, S. McHugh, R. Gonzalez-Rubio, N. Avraham, Y. Myasoedov, E. Zeldov, H. Shtrikman, N.E. Chakov, and G. Christou, Phys. Rev. Lett. **95**, 147201 (2005).

[8] A. Hernandez-Minguez, J.M. Hernandez, F. Macia, A. Garcia-Santiago, J. Tejada, and P.V. Santos, Phys. Rev. Lett. **95**, 217205 (2005).

[9] C. Schlegel, J. van Slageren, M. Manoli, E. K. Brechin, and M. Dressel, Phys. Rev. Lett. **101**, 147203 (2008).

[10] S. Bertaina, S. Gambarelli, T. Mitra, B. Tsukerblat, A. Müller, and B. Barbara, Nature (London) **453**, 203 (2008); ibid **466**, 1006 (2010).

[11] M. Ganzhorn, S. Klyatskaya, M. Ruben, and W. Wernsdorfer, Nat. Nano. **8**, 165 (2013).

[12] M. Ganzhorn, S. Klyatskaya, M. Ruben, and W. Wernsdorfer. ACS Nano. **7**, 6225 (2013).

[13] J. Tejada, E. M. Chudnovsky, E. del Barco, J. M. Hernandez, and T. P. Spiller, Nanotech. **12**, 181 (2001).

[14] I. Imaz, F. Luis, C. Carbonera, D. Ruiz-Molinac, and D. Maspoch, Chem. Commun.,1202 (2008).

[15] C. Carbonera, I. Imaz, D. Maspoch, D. Ruiz-Molina, and F. Luis, Inorg. Chim. Acta **361**, 4937 (2008).

[16] F. El Hallak, J. van Slageren, J. Gómez-Segura, D. Ruiz-Molina, and M. Dressel, Phys. Rev. B **75**, 104403 (2007).

[17] C. Carbonera, J. Luis, J. Campo, J. Sánchez-Marcos, A. Camón, J. Chaboy, D. Ruiz-Molina, I. Imaz, J. van Slageren, S. Dengler, and M. Conzález, Phys. Rev. B **81**, 014427 (2010).

[18] P. J. Chupas, X. Qiu, J. C. Hanson, P. L. Lee, C. P. Grey, and S. J. L. Billinge, J. Appl. Crystallogr. **36**, 1342 (2003).

[19] P. Juhas, T. Davis, C. L. Farrow, and S. J. L. Billinge, J. Appl. Crystallogr. **46**, 560 (2013).

[20] P. Langan, R. Robinson, P. J. Brown, D. Argyriou, D. Hendrickson, and G. Christou, Acta Crystallogr. C **57**, 909 (2001).

[21] A. Cornia, A. C. Fabretti, R. Sessoli, L. Sorace, D. Gatteschi, A.-L. Barra, C. Daiguebonne, and T. Roisnel, Acta Crystallogr. C **58**, m371 (2002).

[22] D. R. Nelson, J. Non-Cryst. Solids, **61-62**, 475 (1984).

[23] E. M. Chudnovsky and J. Tejada, Europhys. Lett., **23**, 517 (1993).

[24] M. Mannini, F. Pineider, C. Danieli, F. Totti, L. Sorace, P. Sainctavit, M.-A. Arrio, E. Otero, L. Joly, J. C. Cezar, A. Cornia, and R. Sessoli, Nature **468**, 417 (2010).